A Novel Finite-Element–Numerical-Integration Model for Composite Laminates Supported on Opposite Edges

Tarun Kant
Professor
e-mail: tkant@civil.iitb.ac.in

Sandeep S. Pendhari
Research Scholar
e-mail: spendhari@iitb.ac.in

Yogesh M. Desai
Professor
e-mail: desai@civil.iitb.ac.in

Department of Civil Engineering,
Indian Institute of Technology Bombay,
Powai, Mumbai-400 076,
India

An attempt is made here to devise a new methodology for an integrated stress analysis of laminated composite plates wherein both in-plane and transverse stresses are evaluated simultaneously. The method is based on the governing three-dimensional (3D) partial differential equations (PDEs) of elasticity. A systematic procedure is developed for a case when one of the two in-plane dimensions of the laminate is considered infinitely long (y direction) with no changes in loading and boundary conditions in that direction. The laminate could then be considered in a two-dimensional (2D) state of plane strain in x-z plane. It is here that the governing 2D PDEs are transformed into a coupled system of first-order ordinary differential equations (ODEs) in transverse z direction by introducing partial discretization in the finite inplane direction x. The mathematical model thus reduces to solution of a boundary value problem (BVP) in the transverse z direction in ODEs. This BVP is then transformed into a set of initial value problems (IVPs) so as to use the available efficient and effective numerical integrators for them. Through thickness displacement and stress fields at the finite element discrete nodes are observed to be in excellent agreement with the elasticity solution. A few new results for cross-ply laminates under clamped support conditions are also presented for future reference and also to show the generality of the formulation. [DOI: 10.1115/1.2722770]

Keywords: plane-strain, partial discretization, laminate, boundary value problem, finite element method, numerical integration method

1 Introduction

Composite materials possess ideal engineering properties and therefore these materials are used in many engineering fields. A three-dimensional (3D) elasticity solution of laminated composite beams or plates or shells is extremely complex. Pagano [1–3], Srinivas and Rao [4], and Srinivas et al. [5] have given flexure, vibration, and buckling response of simply-supported rectangular plates and laminates by analytically solving the governing boundary value problem (BVP) defined by 3D partial differential equations (PDEs). However, these solutions lack generality. Their solutions have been used, over the last three decades, as benchmark solutions by researchers involved in developing general numerical techniques and also by those concerned with the range of applicability of the approximate two-dimensional (2D) plate/shell and one-dimensional (1D) beam/arch theories [6–23]. Accurate estimation of interlaminar stresses is a major concern in the design of laminated composites to avoid delamination. In the available approaches [24], the in-plane stresses are first computed in the first phase of any general laminate analysis. The transverse interlaminar stresses are then estimated by integrating the 3D elasticity equilibrium equations in the second post-processing phase, but serious computational and analytical problems are associated with this second post-processing phase involving accuracy and inconsistency of mathematical model itself.

Taking a cue from the foregoing development, an attempt is made here to extend the strategy of transforming the governing system of PDEs to a system of ODEs for elastostatic problems whose behavior is mathematically formulated as a two-point BVP governed by a set of linear first-order ordinary differential equations (ODEs)

$$\frac{d}{dz}\mathbf{y}(z) = \mathbf{A}(z)\mathbf{y}(z) + \mathbf{p}(z) \tag{1}$$

in the domain $z_1 < z < z_2$.

BVP in ODEs, not only describe one-dimensional (1D) elastostatic problems exactly but also 2D and 3D problems approximately whose behavior is governed by a system of PDEs. Conceptualizing a finite element (FE) discretization in the lamina plane, a set of implicit first-order ODEs is obtained. The solution vector $\mathbf{y}(z)$ of which consists of a set of primary dependent variables (stress components and the corresponding displacements on the lamina plane) whose number equals the order of the PDE system times the number of discrete FE mesh nodes. Availability of efficient, accurate, and, above all, proven robust ODE numerical integrators for IVPs helps in obtaining the set of primary variables at all nodal points through the thickness. Ingenuity lies here in transforming the BVP into a set of initial value problems (IVPs) [25]. Furthermore, the secondary set of dependent variables over the entire nodal set is simply computed by substitution of the values of the primary variables on the right hand side of algebraic expressions, node by node.

2 Partial Discretization Formulation

A laminate supported on two opposite edges $x=0$, a, and loaded transversely by distributed load, which is independent of y is considered. The dimension of the laminate in the y direction is infinite. The thickness h is composed of a number of isotropic and/or orthotropic layers bonded together and whose principal material

Contributed by the Applied Mechanics Division of ASME for publication in the Journal of Applied Mechanics. Manuscript received May 3, 2006; final manuscript received January 3, 2007. Review conducted by Sanjay Govindjee.

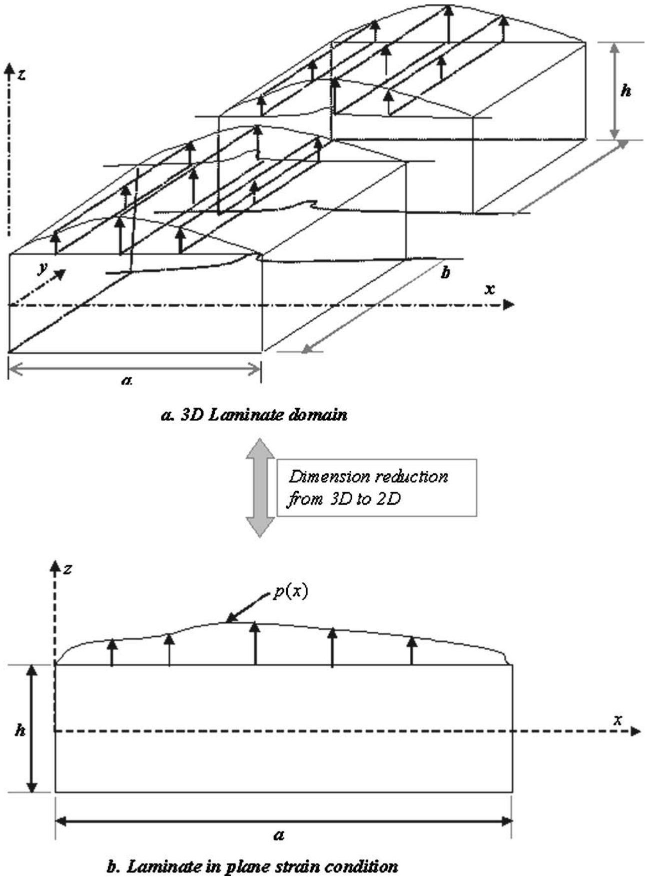

Fig. 1 Laminate subjected to transverse loading

directions are coincident with the geometrical coordinate axis. Under such a condition, the laminate is in a 2D state of plane strain in *x-z* plane (Fig. 1).

The 2D differential equations of equilibrium are

$$\frac{\partial \sigma_x}{\partial x} + \frac{\partial \tau_{zx}}{\partial z} + B_x = 0$$

$$\frac{\partial \tau_{xz}}{\partial x} + \frac{\partial \sigma_z}{\partial z} + B_z = 0 \tag{2}$$

where B_x and B_z are the body forces per unit volume in x and z directions, respectively.

The material constitute relations for each layer can be written as

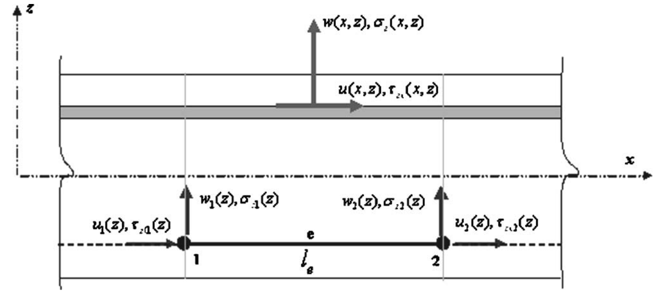

Fig. 2 Linear finite element with dependent variables

$$\begin{Bmatrix} \sigma_x \\ \sigma_z \\ \tau_{zx} \end{Bmatrix} = \begin{bmatrix} C_{11} & C_{12} & 0 \\ C_{21} & C_{22} & 0 \\ 0 & 0 & C_{33} \end{bmatrix} \begin{Bmatrix} \varepsilon_x \\ \varepsilon_z \\ \gamma_{zx} \end{Bmatrix} \tag{3}$$

The stiffness coefficients C_{ij} are the elastic constants derived by setting $\varepsilon_y = \gamma_{xy} = \gamma_{yz} = 0$ in the 3D material stiffness matrix and are given in the Appendix. The general linear strain-displacement relations in 2D can be written as,

$$\varepsilon_x = \frac{\partial u}{\partial x}, \quad \varepsilon_z = \frac{\partial w}{\partial z}, \quad \text{and} \quad \gamma_{zx} = \frac{\partial u}{\partial z} + \frac{\partial w}{\partial x} \tag{4}$$

Equations (2)–(4) have eight unknowns, u, w, ε_x, ε_z, γ_{zx}, σ_x, σ_z, and τ_{zx}. It is to be noted that continuity of transverse stresses and the displacement fields (Fig. 2) are the essential requirements for the accurate analysis of layered components [1–3]. These conditions are naturally enforced in the present formulation. Through a simple algebraic manipulation of the above three sets of Eqs. (2)–(4), a system of PDEs involving four dependent variables $u, w, \tau_{zx}, \sigma_z$ are obtained as follows:

$$\frac{\partial u}{\partial z} = \frac{\tau_{zx}}{C_{33}} - \frac{\partial w}{\partial x}$$

$$\frac{\partial w}{\partial z} = \frac{1}{C_{22}}\left[\sigma_z - C_{21}\frac{\partial u}{\partial x}\right]$$

$$\frac{\partial \tau_{zx}}{\partial z} = \left[-C_{11} + \left(\frac{C_{12}C_{21}}{C_{22}}\right)\right]\frac{\partial^2 u}{\partial x^2} - \frac{C_{12}}{C_{22}}\frac{\partial \sigma_z}{\partial x} - B_x$$

$$\frac{\partial \sigma_z}{\partial z} = -\frac{\partial \tau_{zx}}{\partial x} - B_z \tag{5}$$

This set of dependent variables is called a "primary set," which is naturally defined at a plane z=a constant, and the secondary de-

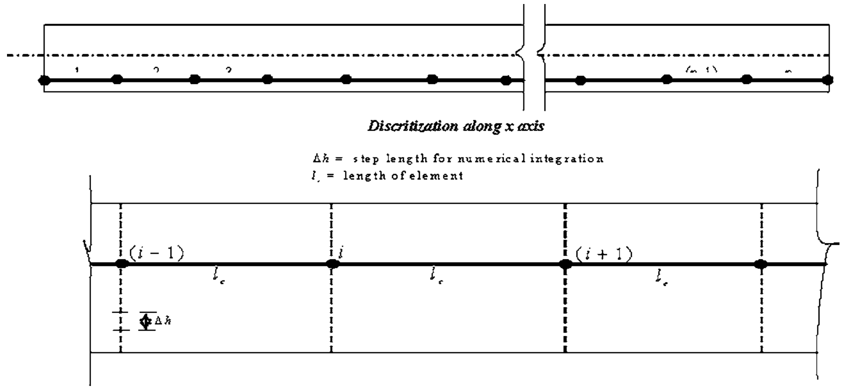

Fig. 3 Linear elements (concept of partial discritization)

Table 1 Boundary conditions (BCs)

Group	Edge	BCs on displacement field	BCs on stress field
A	$x=0$ and a	$w=0$	—
	$x=a/2$	$u=0$	$\tau_{zx}=0$
	$z=h/2$	—	$\sigma_z=p(x)$; $\tau_{zx}=0$
	$z=-h/2$	—	$\sigma_z=0$; $\tau_{zx}=0$
B	$x=0$ and a	$w=0$ and $u=0$	—
	$z=h/2$	—	$\sigma_z=p(x)$; $\tau_{zx}=0$
	$z=-h/2$	—	$\sigma_z=0$; $\tau_{zx}=0$

pendent variable σ_x can simply be expressed as a function of the primary set of variables as follows:

$$\sigma_x=\left(C_{11}-\frac{C_{12}C_{21}}{C_{22}}\right)\frac{\partial u}{\partial x}+\frac{C_{12}}{C_{22}}\sigma_z \tag{6}$$

It is noted that the primary set of variables (u,w,τ_{zx},σ_z) is a function of independent coordinates x and z. It is proposed to carry out FE discretization in only the x direction such that the discrete dependent vector $\mathbf{y}(z)$ will be a only function of independent coordinate z, and a system of coupled discrete first-order ODEs connecting all FE nodes results. This new formulation is described below, first with reference to a two-noded linear element in the x direction with mixed set of primary variables as nodal degrees of freedom (Fig. 2).

The approximate variation of displacements field over the element domain along the longitudinal axis x can be written as

$$u\simeq\hat{u}(x,z)=u_1(z)N_1(x)+u_2(z)N_2(x)$$

$$w\simeq\hat{w}(x,z)=w_1(z)N_1(x)+w_2(z)N_2(x) \tag{7}$$

and from the basic relations of theory of elasticity it can be shown that

$$\tau_{zx}\simeq\hat{\tau}_{zx}(x,z)=\tau_{zx1}(z)N_1(x)+\tau_{zx2}(z)N_2(x)$$

$$\sigma_z\simeq\hat{\sigma}_z(x,z)=\sigma_{z1}(z)N_1(x)+\sigma_{z2}(z)N_2(x) \tag{8}$$

where $N_1=1-(x/l_e)$ and $N_1=x/l_e$.

Substituting Eqs. (7) and (8) into Eq. (5), the domain residuals are obtained as

$$\frac{\partial\hat{u}(x,z)}{\partial z}+\frac{\partial\hat{w}(x,z)}{\partial x}-\frac{\hat{\tau}_{zx}(x,z)}{C_{33}}=R_{1D}(x)$$

$$\frac{\partial\hat{w}(x,z)}{\partial z}+\frac{C_{21}}{C_{22}}\frac{\partial\hat{u}(x,z)}{\partial x}-\frac{\hat{\sigma}_z(x,z)}{C_{22}}=R_{2D}(x)$$

$$\frac{\partial\hat{\tau}_{zx}(x,z)}{\partial z}+\left(C_{11}-\frac{C_{12}C_{21}}{C_{22}}\right)\frac{\partial^2\hat{u}(x,z)}{\partial x^2}+\frac{C_{12}}{C_{22}}\frac{\partial\hat{\sigma}_z(x,z)}{\partial x}+\hat{B}_x(x,z)=R_{3D}(x)$$

$$\frac{\partial\hat{\sigma}_z(x,z)}{\partial z}+\frac{\partial\hat{\tau}_{zx}(x,z)}{\partial x}+\hat{B}_z(x,z)=R_{4D}(x) \tag{9}$$

The strong Bubnov-Galerkin weighted residual statements [26] can then be written with the help of Eq. (9) as follows:

$$\int_0^{l_e}N_i(x)\left(\frac{\partial\hat{u}(x,z)}{\partial z}+\frac{\partial\hat{w}(x,z)}{\partial x}-\frac{\hat{\tau}_{zx}(x,z)}{C_{33}}\right)dx=0 \tag{10}$$

$$\int_0^{l_e}N_i(x)\left(\frac{\partial\hat{w}(x,z)}{\partial z}+\frac{C_{21}}{C_{22}}\frac{\partial\hat{u}(x,z)}{\partial x}-\frac{\hat{\sigma}_z(x,z)}{C_{22}}\right)dx=0 \tag{11}$$

$$\int_0^{l_e}N_i(x)\left[\frac{\partial\hat{\tau}_{zx}(x,z)}{\partial z}+\left(C_{11}-\frac{C_{12}C_{21}}{C_{22}}\right)\frac{\partial^2\hat{u}(x,z)}{\partial x^2}+\frac{C_{12}}{C_{22}}\frac{\partial\hat{\sigma}_z(x,z)}{\partial x}+\hat{B}_x(x,z)\right]dx=0 \tag{12}$$

$$\int_0^{l_e}N_i(x)\left(\frac{\partial\hat{\sigma}_z(x,z)}{\partial z}+\frac{\partial\hat{\tau}_{zx}(x,z)}{\partial x}+\hat{B}_z(x,z)\right)dx=0 \tag{13}$$

Equation (12), which contains a second-order derivative of $\hat{u}$, is replaced by its weak form with the help of integration by parts as follows:

$$\int_0^{l_e}N_i(x)\frac{\partial\hat{\tau}_{zx}(x,z)}{\partial z}dx-\int_0^{l_e}\frac{dN_i(x)}{dx}\left(C_{11}-\frac{C_{12}C_{21}}{C_{22}}\right)\frac{\partial\hat{u}(x,z)}{\partial x}dx+\int_0^{l_e}N_i(x)\frac{C_{12}}{C_{22}}\frac{\partial\hat{\sigma}_z(x,z)}{\partial x}dx+\left[N_i(x)\left(C_{11}-\frac{C_{12}C_{21}}{C_{22}}\right)\frac{\partial\hat{u}(x,z)}{\partial x}\right]_0^{l_e}+\int_0^{l_e}N_i(x)\hat{B}_x(x,z)dx=0 \tag{14}$$

On substitution for approximate functions from Eqs. (7) and (8), the following eight semi-discrete equations are obtained:

$$\begin{bmatrix} A_{11}^e & 0 & 0 & 0 & A_{15}^e & 0 & 0 & 0\\ 0 & A_{22}^e & 0 & 0 & 0 & A_{26}^e & 0 & 0\\ 0 & 0 & A_{33}^e & 0 & 0 & 0 & A_{37}^e & 0\\ 0 & 0 & 0 & A_{44}^e & 0 & 0 & 0 & A_{48}^e\\ A_{51}^e & 0 & 0 & 0 & A_{55}^e & 0 & 0 & 0\\ 0 & A_{62}^e & 0 & 0 & 0 & A_{66}^e & 0 & 0\\ 0 & 0 & A_{73}^e & 0 & 0 & 0 & A_{77}^e & 0\\ 0 & 0 & 0 & A_{84}^e & 0 & 0 & 0 & A_{88}^e \end{bmatrix}\frac{d}{dz}\begin{Bmatrix} u_1^e(z)\\ w_1^e(z)\\ \tau_{zx1}^e(z)\\ \sigma_{z1}^e(z)\\ u_2^e(z)\\ w_2^e(z)\\ \tau_{zx2}^e(z)\\ \sigma_{z2}^e(z)\end{Bmatrix}$$

$$=\begin{bmatrix} 0 & B_{12}^e & B_{13}^e & 0 & 0 & B_{16}^e & B_{17}^e & 0\\ B_{21}^e & 0 & 0 & B_{24}^e & B_{25}^e & 0 & 0 & B_{28}^e\\ B_{31}^e & 0 & 0 & B_{34}^e & B_{35}^e & 0 & 0 & B_{38}^e\\ 0 & 0 & B_{43}^e & 0 & 0 & 0 & B_{47}^e & 0\\ 0 & B_{52}^e & B_{53}^e & 0 & 0 & B_{56}^e & B_{57}^e & 0\\ B_{61}^e & 0 & 0 & B_{64}^e & B_{65}^e & 0 & 0 & B_{68}^e\\ B_{71}^e & 0 & 0 & B_{74}^e & B_{75}^e & 0 & 0 & B_{78}^e\\ 0 & 0 & B_{83}^e & 0 & 0 & 0 & B_{87}^e & 0 \end{bmatrix}\begin{Bmatrix} u_1^e(z)\\ w_1^e(z)\\ \tau_{zx1}^e(z)\\ \sigma_{z1}^e(z)\\ u_2^e(z)\\ w_2^e(z)\\ \tau_{zx2}^e(z)\\ \sigma_{z2}^e(z)\end{Bmatrix}+\begin{Bmatrix}0\\0\\p_3^e\\p_4^e\\0\\0\\p_7^e\\p_8^e\end{Bmatrix}$$

which can be written in a compact form as

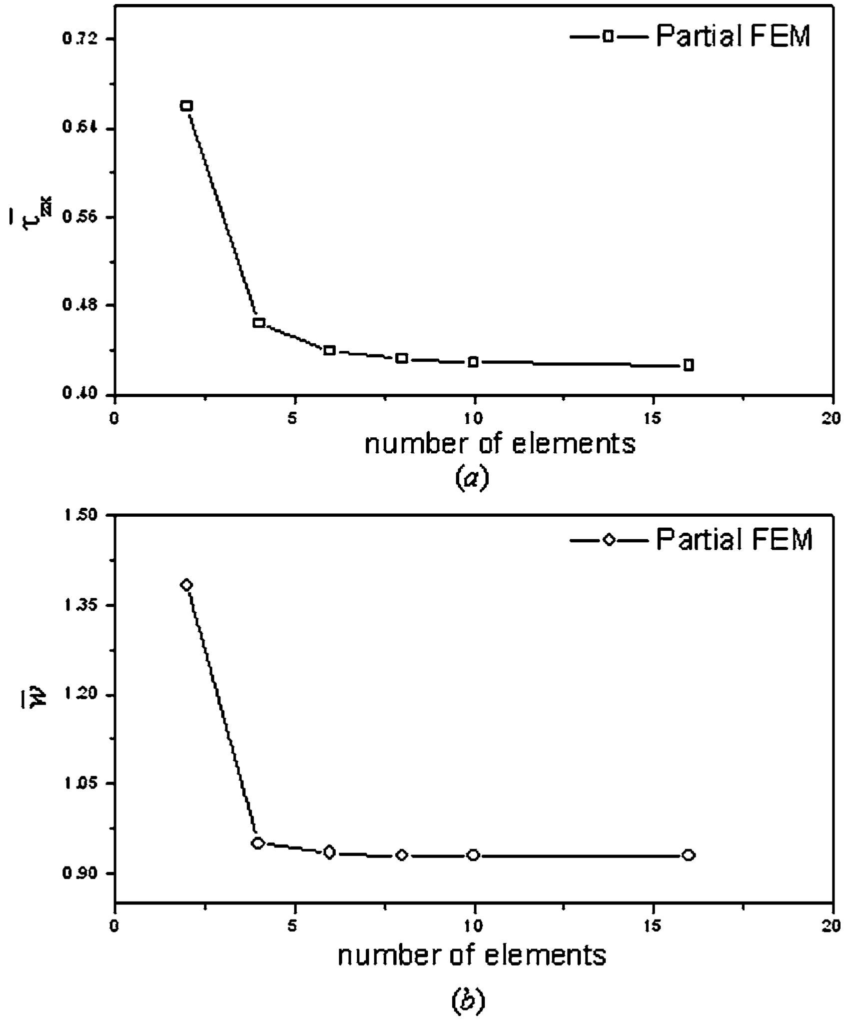

Fig. 4 Convergence of (*a*) maximum transverse shear stress ($\overline{\tau_{zx}}$) and (*b*) mid-plane transverse displacement ($\bar{w}$) with number of elements for a 0 deg/90 deg/0 deg laminate under cylindrical bending

$$A^e(x)\frac{d}{dz}\boldsymbol{y}^e(z) = \mathbf{B}^e(x,z)\boldsymbol{y}^e(z) + \boldsymbol{p}^e(x,z) \tag{15}$$

The elements of matrices $\mathbf{A}^e(x)$, $\mathbf{B}^e(x,z)$ and vector $\mathbf{p}^e(x,z)$ are given in the Appendix. When the total x dimension is discretized with n two-noded elements (Fig. 3), then the semi-discrete system of equation for the entire domain turns out to be

$$\sum_{k=1}^{n} \mathbf{A}^e(x)\frac{d}{dz}\boldsymbol{y}^e(z) = \sum_{k=1}^{n} \mathbf{B}^e(x,z)\boldsymbol{y}^e(z) + \sum_{k=1}^{n} \boldsymbol{p}^e(x,z)$$

or

$$\mathbf{A}(x)\frac{d}{dz}\boldsymbol{y}(z) = \mathbf{B}(x,z)\boldsymbol{y}(z) + \boldsymbol{p}(x,z) \tag{16}$$

Multiplication of Eq. (16) by $[\mathbf{A}(x)]^{-1}$ on both sides results in

$$\frac{d}{dz}\boldsymbol{y}(z) = \mathbf{C}(x,z)\boldsymbol{y}(z) + \boldsymbol{f}(x,z) \tag{17}$$

where $\mathbf{C}(x,z)=[\mathbf{A}(x)]^{-1}\mathbf{B}(x,z)$ and $\boldsymbol{f}(x,z)=[\mathbf{A}(x)]^{-1}\mathbf{p}(x,z)$.

Equation (17) defines the governing equations of a two-point BVP in ODEs in the domain $-(h/2)<z<(h/2)$. $\boldsymbol{y}(z)$ is an m-dimensional (m=number of nodes$\times$4) vector of dependent variables, $\mathbf{C}(x,z)$ is an $m\times m$ coefficient matrix (which is a function of element geometry along x and material properties variation both in the x and z directions), and $f(x,z)$ is an m-dimensional vector of nonhomogeneous (loading) terms. Any $m/2$ elements of $\boldsymbol{y}(z)$ are prescribed at the two ends, $z=-(h/2)$ and $h/2$ as boundary conditions. It is clearly seen that mixed and/or nonhomogeneous boundary conditions are easily admitted in this formulation. The basic approach to the numerical integration of the BVP defined by Eq. (17) is to transform the given BVP into a set of IVPs—one particular (nonhomogeneous) and $m/2$ complimentary (homogeneous). Clearly, the reason behind this is the availability of a number of successful and well-tested algorithms for numerical solution of IVPs in ODEs. The solution of the original BVP defined by Eq. (17) is obtained by forming a linear combination of one nonhomogeneous and $m/2$ homogeneous solutions so as to satisfy the boundary conditions at $z=h/2$. This gives rise to a system of $m/2$ linear algebraic equations, the solution of which determines the unknown $m/2$ components of the vector of initial values $\boldsymbol{y}(z)$. Then a final numerical integration of Eq. (17) with completely known initial vector of dependent variables $\boldsymbol{y}(z)$ produces the desired results. It is intended here to extend the applicability of this procedure, which is documented by Kant and Ramesh [25].

3 Numerical Studies

A two-noded linear element with mixed (displacements/stresses) degrees of freedom is employed in the present numerical

Table 2 Comparison of normalized transverse displacement ($\bar{w}$), in-plane normal stress ($\overline{\sigma_x}$), and transverse shear stress ($\overline{\tau_{zx}}$) of two-layered (0 deg/90 deg) unsymmetric laminates under cylindrical bending

Aspect ratio	Source	Stresses/displacement			
		$\overline{\sigma_x}$ $(a/2,h/2)$	$\overline{\sigma_x}$ $(a/2,-h/2)$	$\overline{\tau_{zx}}$ (0,max)	$\bar{w}$ $(a/2,0)$
4	Partial FEM	0.2325	−1.8142	0.6983	4.6826
		(−3.0037)	(−3.3355)	(2.6157)	(−0.2705)
	Pagano [1][a]	0.2397	−1.8768	0.6805	4.6953
	Enhblom and Ochoa [9]	0.1864	−1.7371	N/A	N/A
	Lu and Liu [13]	0.2232	−1.8750	N/A	4.7773
10	Partial FEM	0.1952	−1.7403	0.7343	2.9503
		(−1.5633)	(−1.4162)	(1.0319)	(−0.1185)
	Pagano [1][a]	0.1983	−1.7653	0.7268	2.9538
	Lu and Liu [13]	0.2000	−1.7500	N/A	3.0000
20	Partial FEM	0.1890	−1.7241	0.7432	2.6980
		(−1.3570)	(−1.4405)	(1.1432)	(−0.1739)
	Pagano [1][a]	0.1916	−1.7493	0.7348	2.7027
50	Partial FEM	0.1866	−1.7196	0.7465	2.6267
		(−1.6341)	(−1.4500)	(1.2752)	(−0.2127)
	Pagano [1][a]	0.1897	−1.7449	0.7371	2.6323

[a]The analytical solution given in this paper is programed by the present authors and numerical results for various aspect ratios, not available in the original paper are obtained and presented here.
N/A=results are not available.

study involving both validation and solution of new problems. A computer code incorporating the present methodology was developed in FORTRAN-90. The accuracy of the proposed new formulation for layered composites is established by comparison of the present numerical results with that of elasticity solution [1] and also with others. In all the examples, the layer elastic coefficients are those of a unidirectional graphite/epoxy composite

$$\mathbf{E_L} = 25 \times 10^6 \text{ psi}; \quad \mathbf{E_T} = 10^6 \text{ psi}; \quad \mathbf{G_{LT}} = 0.5 \times 10^6 \text{ psi}$$

$$\mathbf{G_{TT}} = 0.2 \times 10^6 \text{ psi}; \quad \boldsymbol{\nu}_{\mathbf{LT}} = \boldsymbol{\nu}_{\mathbf{TT}} = 0.25$$

where subscripts **L** and **T** refer to the fiber direction and transverse direction perpendicular to fiber direction.

Two support conditions on opposite edges considered here are tabulated in Table 1. All laminates are subjected to sinusoidal transverse load on their top surface. The intensity of sinusoidal loading can be expressed as

$$p(x) = p_0 \sin \frac{\pi x}{a} \tag{18}$$

where p_0 represents the peak intensity of load.

The dependent quantities are nondimensionalized in the following manner:

Table 3 Comparison of normalized transverse displacement ($\bar{w}$), in-plane normal stress ($\overline{\sigma_x}$), and transverse shear stress ($\overline{\tau_{zx}}$) of three-layered (0 deg/90 deg/0 deg) symmetric laminates under cylindrical bending

Aspect ratio	Source	Stresses/displacement			
		$\overline{\sigma_x}$ $(a/2,h/2)$	$\overline{\sigma_x}$ $(a/2,-h/2)$	$\overline{\tau_{zx}}$ (0,max)	$\bar{w}$ $(a/2,0)$
4	Partial FEM	1.1211	−1.0782	0.4149	2.9134
		(−4.6278)	(−4.7105)	(4.8522)	(0.9074)
	Pagano [1][a]	1.1755	−1.1315	0.3957	2.8872
	Spilker [8]	N/A	N/A	0.3909	2.8410
	Enhblom and Ochoa [9]	0.6256	−0.6318	0.4434	N/A
10	Partial FEM	0.7216	−0.7211	0.4285	0.9308
		(−2.049)	(−2.0644)	(1.0851)	(−0.0859)
	Pagano [1][a]	0.7367	−0.7363	0.4239	0.9316
	Spilker [8]	N/A	N/A	0.4529	0.9312
	Enhblom and Ochoa [9]	0.6373	−0.6373	0.4459	N/A
20	Partial FEM	0.6439	−0.6440	0.4431	0.6152
		(−2.1280)	(−2.1425)	(1.3031)	(−0.3240)
	Pagano [1][a]	0.6579	−0.6581	0.4374	0.6172
50	Partial FEM	0.6211	−0.6211	0.4483	0.5246
		(−2.1581)	(−2.1581)	(1.5402)	(−0.4554)
	Pagano [1][a]	0.6348	−0.6348	0.4415	0.5270

[a]The analytical solution given in this paper is programmed by the present authors and numerical results for various aspect ratios, not available in the original paper are obtained and presented here.
N/A=results are not available.

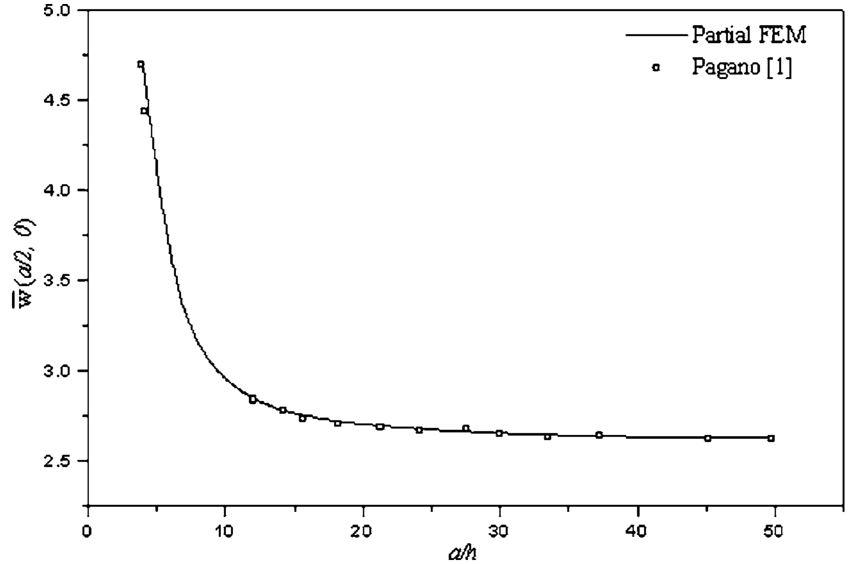

Fig. 5 Variation of normalized transverse displacement ($\bar{w}$) with respect to *a*/*h* ratios of 0 deg/90 deg unsymmetric laminates under cylindrical bending

$$\bar{z} = \frac{z}{h}; \quad \bar{u} = \frac{E_2 u(0,z)}{hp_0}; \quad \bar{w} = \frac{100E_2 h^3 w(a/2,0)}{p_0 a^4}$$

$$\overline{\sigma_x} = \frac{h^2 \sigma_x(a/2,0)}{p_0 a^2}; \quad \overline{\sigma_z} = \frac{\sigma_z(a/2,z)}{p_0}; \quad \overline{\tau_{zx}} = \frac{h\tau_{xz}(0,z)}{p_0 a} \qquad (19)$$

in which a bar over a variable defines its nondimensionalized value and the percentage error between present and elasticity solution [1] is calculated as

$$\%\ \text{error} = \frac{\text{Present analysis} - \text{Elasticity solution}}{\text{Elasticity solution}} \times 100 \qquad (20)$$

and these are presented in parentheses in Table 1.

A convergence study on number of elements along the x direction and number of steps required for numerical integration in thickness direction is performed first. The method was found to yield converged solution for a laminates in-plane strain with 12–16 elements in the x direction and with 16–20 steps in the thickness, z direction. Convergence plot of midplane transverse displacement ($\bar{w}$) and maximum transverse shear stress ($\overline{\tau_{zx}}$) with the number of elements in the x direction are shown graphically for the symmetric (0 deg/90 deg/0 deg) laminates in Fig. 4 for a/h ratio of 10.

Group A. The examples considered in this group are selected to establish the accuracy of stress predictions through the thickness by the present method. A two-layer unsymmetric (0 deg/90 deg) and a three-layer symmetric (0 deg/90 deg/0 deg) cross-ply square laminates, simply supported on opposite edges in the x direction are considered for this purpose. Boundary conditions are specified in Table 1. The results obtained through present analysis are compared to the 3D elasticity solution given by Pagano [1] and also with available results in the literature [8,9,13] for cylindrical bending. Numerical results for a/h ratios of 4, 10, 20, and 50 are given in Tables 2 and 3 for both configurations. The variation of midplane transverse displacement $\bar{w}(a/2,0)$ with different a/h ratios is shown in Fig. 5. Through thickness variation of normalized in-plane normal stress ($\overline{\sigma_x}$), inplane displacement ($\bar{u}$), transverse shear stress ($\overline{\tau_{xz}}$) and transverse normal stress ($\overline{\sigma_z}$) for a/h ratio of 4 are presented in Figs. 6 and 7 for 0 deg/90 deg unsymmetric laminate and 0 deg/90 deg/0 deg symmetric laminate, respectively. Moreover, through thickness variation of transverse displacement ($\bar{w}$) is depicted in Fig. 8. Excellent agreement is seen between the present and the elasticity solution.

Group B. The examples considered under this group are an extension of group A for clamped end conditions to show the ability of the present formulation to handle problems with general boundary conditions and high stress gradients. The lamination schemes, material properties and geometrical details are kept same as group A. Boundary conditions are specified in Table 1. Numerical results for normal in-plane stress ($\overline{\sigma_x}$) at top and bottom, transverse shear stress ($\overline{\tau_{xz}}$), and transverse displacement ($\bar{w}$) at midplane with different a/h ratios are presented in Table 4 for both 0 deg/90 deg unsymmetric and 0 deg/90 deg/0 deg symmetric laminates. The normal in-plane stress ($\overline{\sigma_x}$) and transverse shear stress ($\overline{\tau_{xz}}$) variations through thickness of laminate with a/h ratio of 4 are shown graphically in Figs. 9 and 10 for 0 deg/90 deg unsymmetric and 0 deg/90 deg/0 deg symmetric laminates, respectively. These results should serve as benchmark solutions for future investigation.

4 Concluding Remarks

A novel partial discretization method with mixed degrees of freedom has been proposed in this paper. It ensures the fundamental elasticity relationship between stress, strain, and displacement fields within the elastic continuum and implicitly maintains the continuity of displacements and transverse stresses at the laminate interface. It is first of its kind of a mixed partial FE model that is based on the solution of a two-point BVP through the thickness of laminates. Good agreement of the results with the elasticity solution suggests that the method is extremely accurate. Generality of the method is proven by incorporation of clamped edge conditions at $x=0$, a. The most significant advantage of the present formulation lies in the fact that both displacement and transverse interlaminar stresses are simultaneously evaluated at the finite element node with the same degree of accuracy through a numerical integration process and thus eliminating the post-processing module that is required in other analytical models for calculation of transverse stresses from in-plane stresses.

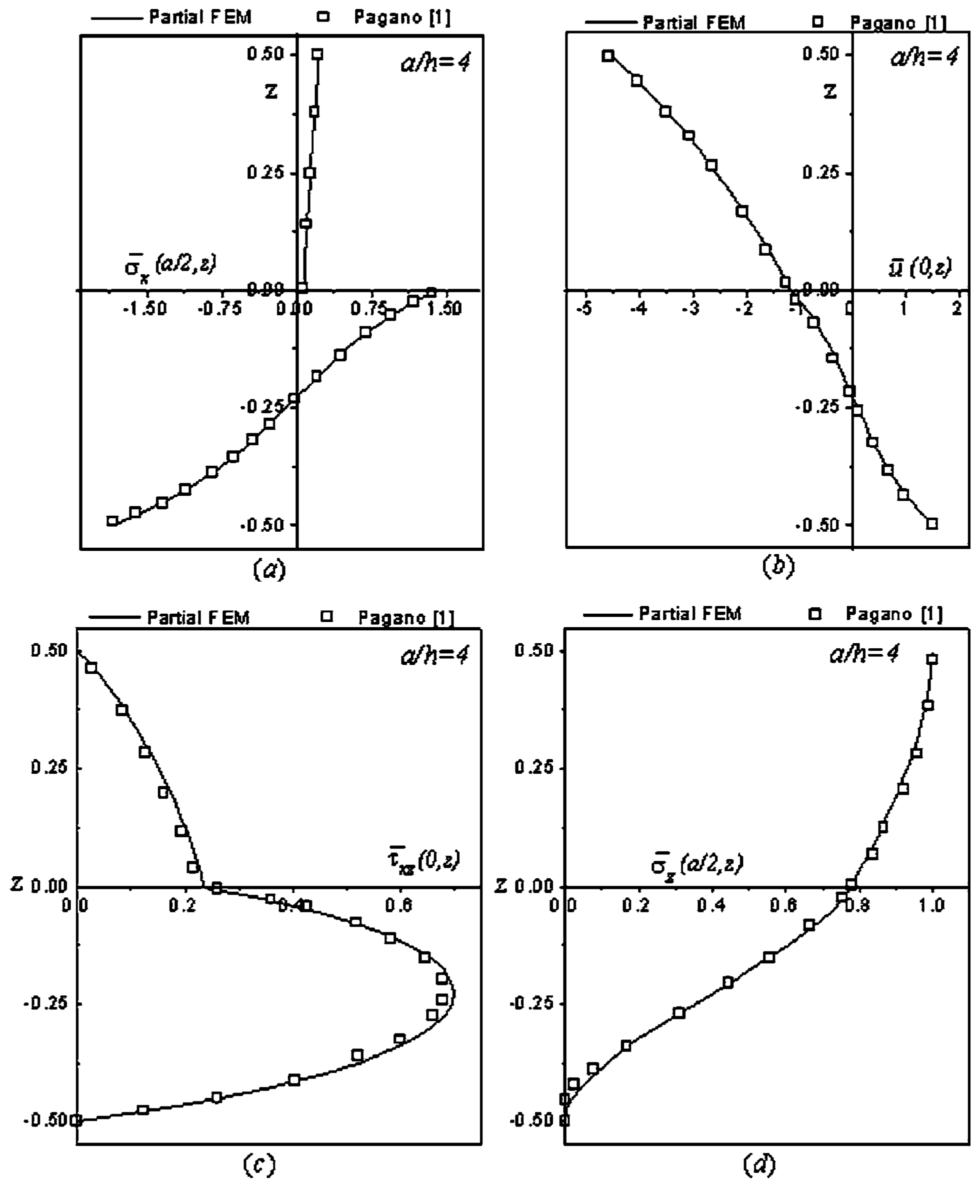

Fig. 6 Variation of normalized (*a*) in-plane normal stress $\overline{\sigma_x}$, (*b*) in-plane displacement $\bar{u}$, (*c*) transverse shear stress $\overline{\tau_{zx}}$, and (*d*) transverse normal stress $\overline{\sigma_z}$ through thickness of 0 deg/90 deg unsymmetric laminate under cylindrical bending

Acknowledgment

Partial support of USIF Indo-US Collaborative Sponsored Research Project No. IND104 (95IU001) is gratefully acknowledged.

Appendix

The stiffness coefficients C_{ij}

$$C_{11} = \frac{E_1(1 - \upsilon_{23}\upsilon_{32})}{\Delta}$$

$$C_{12} = C_{21} = \frac{E_1(\upsilon_{21} + \upsilon_{31}\upsilon_{23})}{\Delta}$$

$$C_{22} = \frac{E_2(1 - \upsilon_{13}\upsilon_{31})}{\Delta}$$

$$C_{33} = G_{xz}$$

were $\Delta = (1 - \upsilon_{12}\upsilon_{21} - \upsilon_{13}\upsilon_{31} - \upsilon_{23}\upsilon_{32} - 2\upsilon_{12}\upsilon_{31}\upsilon_{23})$, E_i=Young's moduli of lamina in the material principle direction $(i=1,2,3)$, and υ_{ij}=generalized Poisson's ratios of lamina $(i,j=1,2,3)$.

Elements of matrix $A^e(x)$ are

$$A^e_{11} = A^e_{22} = A^e_{33} = A^e_{44} = A^e_{55} = A^e_{66} = A^e_{77} = A^e_{88} = \int_0^{l_e} N_1(x)N_1(x)dx$$

$$= \frac{l_e}{3}$$

$$A^e_{15} = A^e_{26} = A^e_{37} = A^e_{48} = A^e_{51} = A^e_{62} = A^e_{73} = A^e_{84} = \int_0^{l_e} N_1(x)N_2(x)dx$$

$$= \frac{l_e}{6}$$

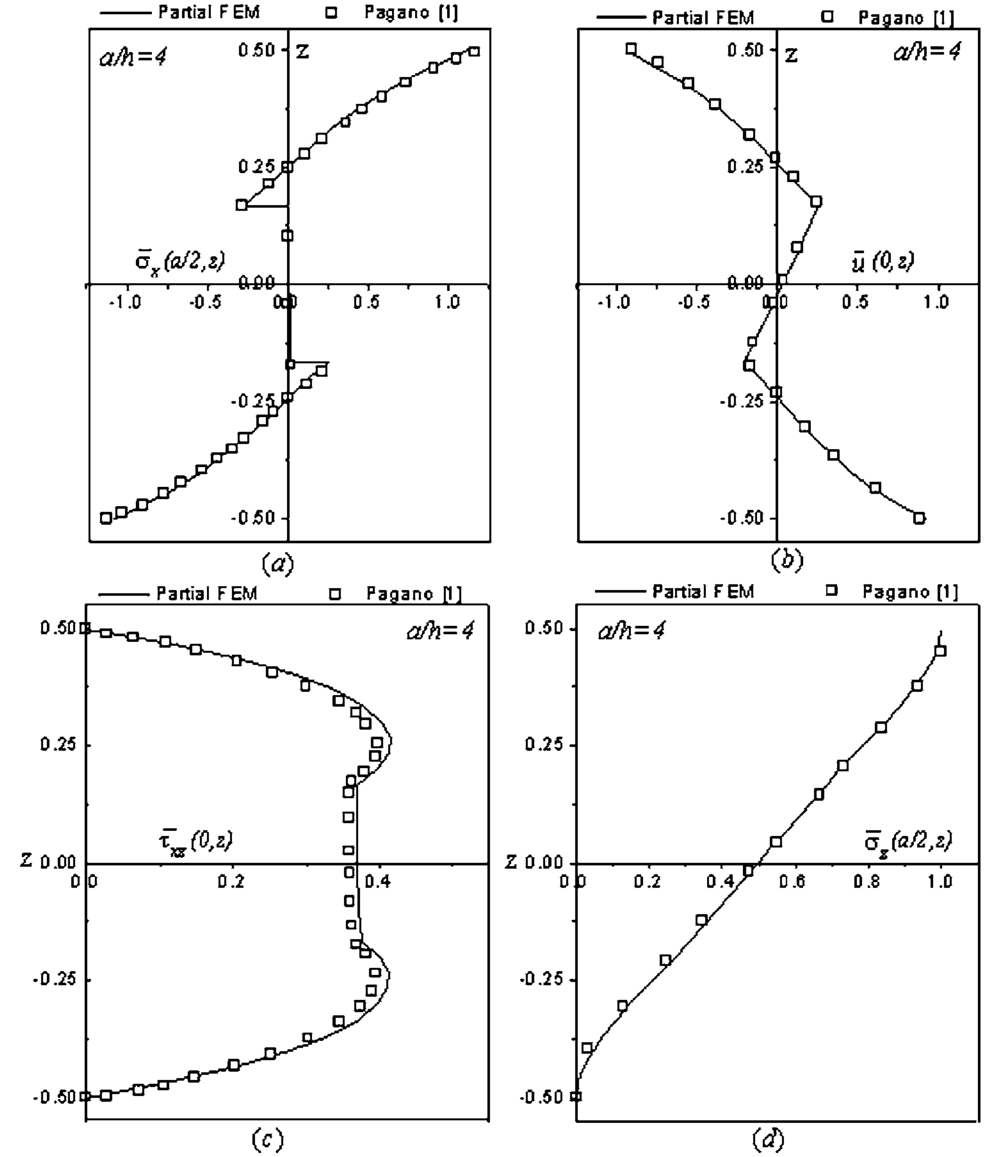

Fig. 7 Variation of normalized (*a*) inplane normal stress $\overline{\sigma_x}$, (*b*) inplane displacement $\bar{u}$, (*c*) transverse shear stress $\overline{\tau_{zx}}$, and (*d*) transverse normal stress $\overline{\sigma_z}$ through thickness of 0 deg/90 deg/0 deg symmetric laminate under cylindrical bending

Elements of matrix $B^e(x,z)$ are

$$B_{12}^e = -\int_0^{l_e} N_1(x)\frac{dN_1(x)}{dx}dx = \frac{1}{2}$$

$$B_{13}^e = \frac{1}{C_{33}}\int_0^{l_e} N_1(x)N_1(x)dx = \frac{l_e}{3C_{33}}$$

$$B_{16}^e = -\int_0^{l_e} N_1(x)\frac{dN_2(x)}{dx}dx = -\frac{1}{2}$$

$$B_{17}^e = \frac{1}{C_{33}}\int_0^{l_e} N_1(x)N_2(x)dx = \frac{l_e}{6C_{33}}$$

$$B_{21}^e = -\frac{C_{21}}{C_{22}}\int_0^{l_e} N_1(x)\frac{dN_1(x)}{dx}dx = \frac{C_{31}}{2C_{22}}$$

$$B_{24}^e = \frac{1}{C_{22}}\int_0^{l_e} N_1(x)N_1(x)dx = \frac{l_e}{3C_{22}}$$

$$B_{25}^e = -\frac{C_{21}}{C_{22}}\int_0^{l_e} N_1(x)\frac{dN_2(x)}{dx}dx = -\frac{C_{21}}{2C_{22}}$$

$$B_{28}^e = \frac{1}{C_{22}}\int_0^{l_e} N_1(x)N_2(x)dx = \frac{l_e}{6C_{22}}$$

$$B_{31}^e = \left(C_{11} - \frac{C_{12}C_{21}}{C_{22}}\right)\int_0^{l_e} \frac{dN_1(x)}{dx}\frac{dN_1(x)}{dx}dx = \left(C_{11} - \frac{C_{12}C_{21}}{C_{22}}\right)\frac{1}{l_e}$$

$$B_{34}^e = -\frac{C_{12}}{C_{22}}\int_0^{l_e} N_1\frac{dN_1(x)}{dx}dx = \frac{C_{12}}{2C_{22}}$$

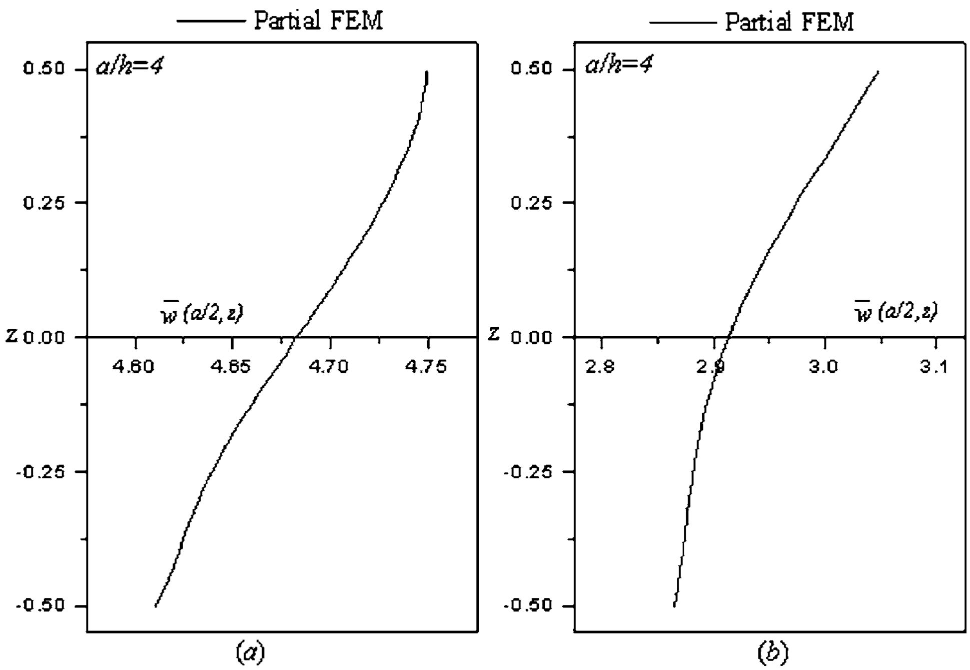

Fig. 8 Variation of normalized transverse displacement $\bar{w}$ through thickness of (*a*) 0 deg/90 deg unsymmetric and (*b*) 0 deg/90 deg/0 deg symmetric laminates under cylindrical bending

$$B_{35}^e = \left(C_{11} - \frac{C_{12}C_{21}}{C_{22}}\right)\int_0^{l_e} \frac{dN_1(x)}{dx}\frac{dN_2(x)}{dx}dx = -\left(C_{11} - \frac{C_{12}C_{21}}{C_{22}}\right)\frac{1}{l_e}$$

$$B_{38}^e = -\frac{C_{12}}{C_{22}}\int_0^{l_e} N_1(x)\frac{dN_2(x)}{dx}dx = -\frac{C_{12}}{2C_{22}}$$

$$B_{43}^e = -\int_0^{l_e} N_1(x)\frac{dN_1(x)}{dx}dx = \frac{1}{2}$$

$$B_{47}^e = -\int_0^{l_e} N_1(x)\frac{dN_2(x)}{dx}dx = -\frac{1}{2}$$

$$B_{52}^e = -\int_0^{l_e} N_2(x)\frac{dN_1(x)}{dx}dx = \frac{1}{2}$$

$$B_{53}^e = \frac{1}{C_{33}}\int_0^{l_e} N_2(x)N_1(x)dx = \frac{l_e}{6C_{33}}$$

$$B_{56}^e = -\int_0^{l_e} N_2(x)\frac{dN_2(x)}{dx}dx = -\frac{1}{2}$$

$$B_{57}^e = \frac{1}{C_{33}}\int_0^{l_e} N_2(x)N_2(x)dx = \frac{l_e}{3C_{33}}$$

$$B_{61}^e = -\frac{C_{21}}{C_{22}}\int_0^{l_e} N_2(x)\frac{dN_1(x)}{dx}dx = \frac{C_{21}}{2C_{22}}$$

$$B_{64}^e = \frac{1}{C_{22}}\int_0^{l_e} N_2(x)N_1(x)dx = \frac{l_e}{6C_{22}}$$

$$B_{65}^e = -\frac{C_{21}}{C_{22}}\int_0^{l_e} N_2(x)\frac{dN_2}{dx}(x)dx = -\frac{C_{21}}{2C_{22}}$$

$$B_{68}^e = \frac{1}{C_{22}}\int_0^{l_e} N_2(x)N_2(x)dx = \frac{l_e}{3C_{22}}$$

Table 4 Normalized transverse displacement ($\bar{w}$), in-plane normal stress ($\overline{\sigma_x}$), and transverse shear stress ($\overline{\tau_{zx}}$) of laminates under clamped support condition in-plane strain condition

		Stresses/displacement							
		0 deg/90 deg unsymmetric laminate				0 deg/90 deg/0 deg symmetric laminate			
Aspect ratio	Source	$\overline{\sigma_x}$ $(a/2,h/2)$	$\overline{\sigma_x}$ $(a/2,-h/2)$	$\overline{\tau_{zx}}$ (0,max)	$\bar{w}$ $(a/2,0)$	$\overline{\sigma_x}$ $(a/2,h/2)$	$\overline{\sigma_x}$ $(a/2,-h/2)$	$\overline{\tau_{zx}}$ (0,max)	$\bar{w}$ $(a/2,0)$
4	Partial FEM	0.1241	−0.8041	1.4232	2.7930	0.5511	−0.5166	0.8833	2.0886
10	Partial FEM	0.0909	−0.6697	2.8418	1.0623	0.3320	−0.3304	1.5079	0.4898
20	Partial FEM	0.0739	−0.5956	2.6678	0.6792	0.2428	−0.2424	1.5624	0.2007
50	Partial FEM	0.0649	−0.5746	2.3424	0.5225	0.2065	−0.2064	1.6142	0.1083

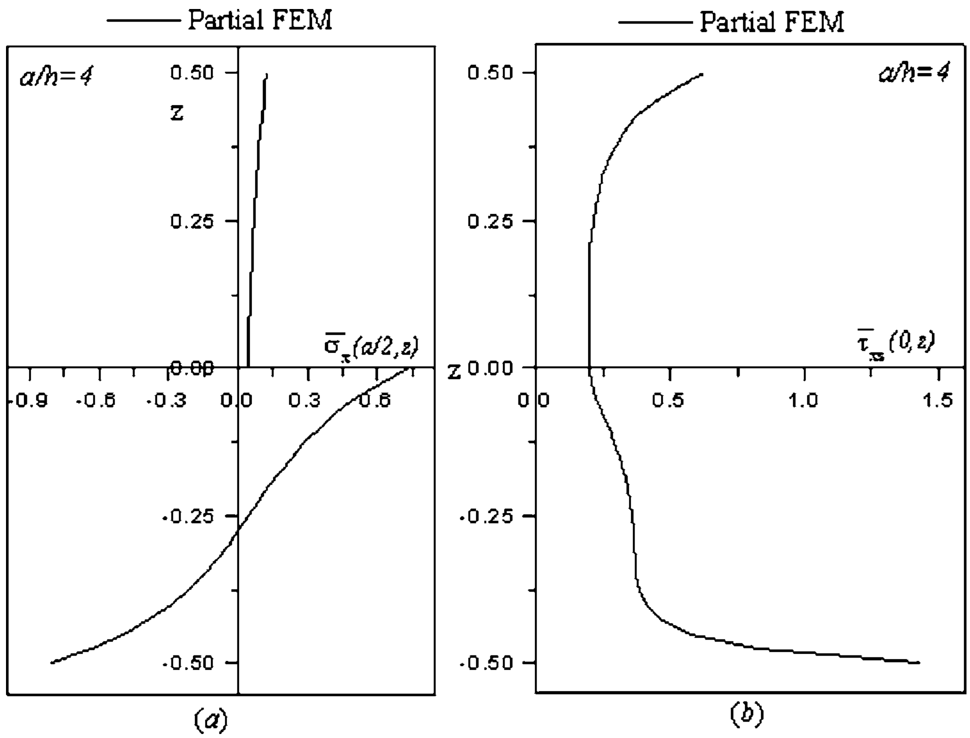

Fig. 9 Variation of normalized (*a*) in-plane normal stress $\overline{\sigma_x}$ and (*b*) transverse shear stress $\overline{\tau_{zx}}$ through thickness of 0 deg/90 deg unsymmetric laminate for clamped supported boundary conditions

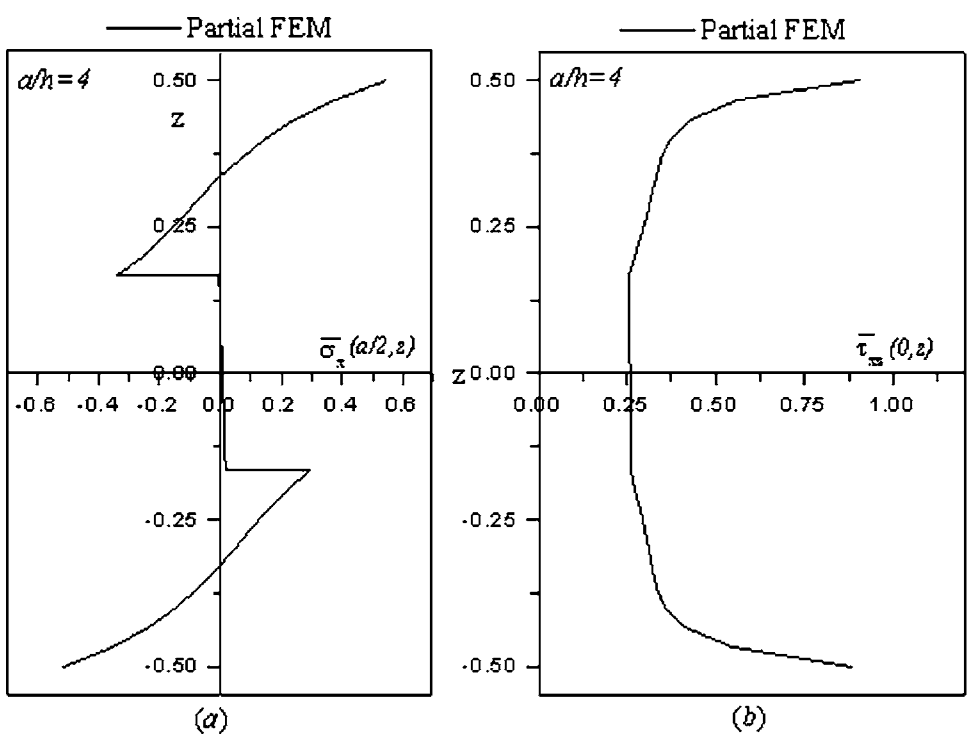

Fig. 10 Variation of normalized (*a*) in-plane normal stress $\overline{\sigma_x}$ and (*b*) transverse shear stress $\overline{\tau_{zx}}$ through thickness of 0 deg/90 deg/0 deg symmetric laminate for clamped supported boundary conditions

$$B_{71}^e = \left(C_{11} - \frac{C_{12}C_{21}}{C_{22}}\right)\int_0^{l_e} \frac{dN_2(x)}{dx}\frac{dN_1(x)}{dx}dx = -\left(C_{11} - \frac{C_{12}C_{21}}{C_{22}}\right)\frac{1}{l_e}$$

$$B_{74}^e = -\frac{C_{12}}{C_{22}}\int_0^{l_e} N_2(x)\frac{dN_1(x)}{dx}dx = \frac{C_{12}}{2C_{22}}$$

$$B_{75}^e = \left(C_{11} - \frac{C_{12}C_{21}}{C_{22}}\right)\int_0^{l_e} \frac{dN_2(x)}{dx}\frac{dN_2(x)}{dx}dx = \left(C_{11} - \frac{C_{12}C_{21}}{C_{22}}\right)\frac{1}{l_e}$$

$$B_{78}^e = -\frac{C_{12}}{C_{22}}\int_{l_1}^{l_2} N_2(x)\frac{dN_2(x)}{dx}dx = -\frac{C_{12}}{2C_{22}}$$

$$B_{83}^e = -\int_0^{l_e} N_2(x)\frac{dN_1(x)}{dx}dx = \frac{1}{2}$$

$$B_{87}^e = -\int_0^{l_e} N_2(x)\frac{dN_2(x)}{dx}dx = -\frac{1}{2}$$

Elements of vector $p^e(x,z)$ are

$$p_3^e = -\int_0^{l_e} N_1(x)\hat{B}_x(x,z)dx - \left[N_1(x)\left(C_{11} - \frac{C_{12}C_{21}}{C_{22}}\right)\frac{d\hat{u}(x,z)}{dx}\right]_0^{l_e}$$

$$p_4^e = -\int_0^{l_e} N_1(x)\hat{B}_z(x,z)dx$$

$$p_7^e = -\int_0^{l_e} N_2(x)\hat{B}_x(x,z)dx - \left[N_2(x)\left(C_{11} - \frac{C_{12}C_{21}}{C_{22}}\right)\frac{d\hat{u}(x,z)}{dx}\right]_0^{l_e}$$

$$p_8^e = -\int_0^{l_e} N_2(x)\hat{B}_z(x,z)dx$$

References

[1] Pagano, N. J., 1969, "Exact Solution for Composite Laminates in Cylindrical Bending," J. Compos. Mater., **3**, pp. 398–411.

[2] Pagano, N. J., 1970, "Exact Solution for Rectangular Bidirectional Composites and Sandwich Plates," J. Compos. Mater., **4**, pp. 20–34.

[3] Pagano, N. J., 1974, "On the Calculation of Interlaminar Normal Stress in Composite Laminates," J. Compos. Mater., **8**, pp. 65–81.

[4] Srinivas, S., and Rao, A. K., 1970, "Bending, Vibration and Buckling of Simply Supported Thick Orthotropic Rectangular Plates and Laminates," Int. J. Solids Struct., **6**, pp. 1463–1481.

[5] Srinivas, S., Joga Rao, C. V., and Rao, A. K., 1970, "An Exact Analysis for Vibration of Simply Supported Homogeneous and Laminated Thick Rectangular Plates," J. Sound Vib., **12**, pp. 187–199.

[6] Pandya, B. N., and Kant, T., 1988, "Higher Order Shear Deformation Theories for Flexure of Sandwich Plates: Finite Element Evaluations," Int. J. Solids Struct., **24**, pp. 1267–1286.

[7] Lo, K. H., Christensen, R. M., and Wu, E. M., 1977, "A High-Order Theory of Plate Deformation—Part 2: Laminated Plate," ASME J. Appl. Mech., **44**, pp. 669–676.

[8] Spilker, R. L., 1982, "Hybrid-Stress Eight-Node Elements for This and Thick Multilayered Laminated Plates," Int. J. Numer. Methods Eng., **18**, pp. 801–828.

[9] Engblom, J. J., and Ochoa, O., 1985, "Through-the-Thickness Stress Predictions for Laminated Plates of Advanced Composite Materials," Int. J. Numer. Methods Eng., **21**, pp. 1759–1776.

[10] Liou, W., and Sun, C. T., 1987, "A Three-Dimensional Hybrid Stress Isoparametric Element for the Analysis of Laminated Composite Plates," Compos. Struct., **25**, pp. 241–249.

[11] Sciuva, M. D., 1987, "An Improved Shear Deformation Theory for Moderately Thick Multilayered Anisotropic Shells and Plates," ASME J. Appl. Mech., **54**, pp. 589–596.

[12] Noor, A. K., and Burton, W. S., 1989, "Stress and Free Vibration Analyses of Multilayered Composite Plates," Compos. Struct., **11**, pp. 183–204.

[13] Lu, X., and Liu, D., 1992, "An Interlaminar Shear Stress Continuity Theory for Both Thin and Thick Composite Laminates," ASME J. Appl. Mech., **59**, pp. 502–509.

[14] Barbero, E. J., 1992, "A 3-D Finite Element for Laminated Composites With 2-D Kinematic Constrains," Compos. Struct., **45**, pp. 263–271.

[15] Chyou, H. A., Sandhu, R. S., and Butalia, T. S., 1995, "Variational Formulation and Finite Element Implementation of Pagano's Theory of Laminated Plates," Mech. Compos. Mater. Struct., **2**, pp. 111–137.

[16] Pai, P. F., 1995, "A New Look at the Shear Correction Factors and Warping Functions of Anisotropic Laminates," Int. J. Solids Struct., **32**, pp. 2295–2313.

[17] Yong, Y. K., and Cho, Y., 1995, "Higher-Order Partial Hybrid Stress, Finite Element Formulation for Laminated Plate and Shell Analysis," Compos. Struct., **57**, pp. 817–827.

[18] Qi, Y., and Knight, N. F., 1996, "A Refined First-Order Shear Deformation Theory and its Justification by Plane-Strain Bending Problem of Laminated Plates," Int. J. Solids Struct., **33**, pp. 49–64.

[19] Aitharaju, V. R., and Averill, R. C., 1999, "C^0 Zigzag Kinematic Displacement Models for the Analysis of Laminated Composites," Mech. Compos. Mater. Struct., **6**, pp. 31–56.

[20] Carrera, E., 2000, "A Priori vs. a Posteriori Evaluation of Transverse Stresses in Multilayered Orthotropic Plates," Compos. Struct., **48**, pp. 245–260.

[21] Alfano, G., Auricchio, F., Rosati, L., and Sacco, E., 2001, "MITC Finite Elements for Laminated Composite Plates," Int. J. Numer. Methods Eng., **50**, pp. 707–738.

[22] Kant, T., and Swaminathan, K., 2001, "Analytical Solutions for Vibration of Laminated Composite and Sandwich Plates Based on a Higher Order Refined Theory," Compos. Struct., **53**, pp. 73–85.

[23] Kant, T., and Swaminathan, K., 2002, "Analytical Solutions for the Static Analysis of Laminated Composite and Sandwich Plates Based on a Higher Order Refined Theory," Compos. Struct., **56**, pp. 329–344.

[24] Kant, T., and Swaminathan, K., 2000, "Estimation of Transverse/Interlaminar Stresses in Laminated Composites—A Selective Review and Survey of Current Developments," Compos. Struct., **49**, pp. 65–75.

[25] Kant, T., and Ramesh, C. K., 1981, "Numerical Integration of Linear Boundary Value Problems in Solid Mechanics by Segmentation Method," Int. J. Numer. Methods Eng., **17**, pp. 1233–1256.

[26] Zienkiewicz, O. C., and Taylor, R. L., 2005, *The Finite Element Method for Solids and Structural Mechanics*, 6th ed., Elsevier Butterworth Heinemann, Oxford.